

We are IntechOpen, the world's leading publisher of Open Access books Built by scientists, for scientists

6,900

Open access books available

186,000

International authors and editors

200M

Downloads

Our authors are among the

154

Countries delivered to

TOP 1%

most cited scientists

12.2%

Contributors from top 500 universities



WEB OF SCIENCE™

Selection of our books indexed in the Book Citation Index
in Web of Science™ Core Collection (BKCI)

Interested in publishing with us?
Contact book.department@intechopen.com

Numbers displayed above are based on latest data collected.
For more information visit www.intechopen.com



Volume Transmission Hologram Gratings – Basic Properties, Energy Channelizing, Effect of Ambient Temperature and Humidity

O.V. Andreeva, Yu.L. Korzinin and B.G. Manukhin

Additional information is available at the end of the chapter

<http://dx.doi.org/10.5772/54253>

1. Introduction

Volume holograms of thickness on order of 1 mm are of great interest from the viewpoint of experimental research base in the field of three-dimensional holography and provision for practical applications of holography, which are related to creation of elements and devices with properties unrealizable by traditional optical methods.

The field of research into volume holograms is at its development stage: inception and generation of theoretical methods to describe the properties of volume holograms, and recording media to produce the latter, experimental techniques to study the properties of high-selectivity volume holograms and materials for their recording.

The present paper offers the authors' view of such an important problem as classification of volume holograms, which has currently no generally accepted clear-cut principles and terminology; discussion of parameters of volume recording media that have been developed in S.I. Vavilov State Optical Institute, Russia, and show principal directions in the field of design of volume recording media for holography; description of the results of the authors' experiments to study the impact of ambient temperature and humidity on parameters of polymeric hologram gratings.

Special attention is paid to examining the special features of transmission hologram gratings with high values of phase modulation amplitudes; the experimental results are given to confirm the presence of the energy channelizing effect by so-called "strong" transmission holograms.

The described experiments used the volume recording media manufactured in laboratory conditions on the base of silicate glass (photo-thermo-refractive glass) and polymer (materi-

al “Difphen” with phenanthrenequinone in polymethylmethacrylate). The issues, assessments and recommendations in question are dealt with on the basis of many years of the authors’ work with volume media for holography.

2. Classification of volume holograms

2.1. Hologram gratings and holograms of complex wave fields

The hologram classification used in literature proceeds according to a number of distinctive signs that include recording conditions, reconstruction conditions, hologram application, specific features of recording media, radiation sources, and so on. The present work concentrates on such distinctive signs as the interference pattern (IP) structure, defined by spatial parameters of interacting waves, the recording medium geometry, and the relationship between them. From this viewpoint, one distinguishes, first of all, hologram gratings and holograms of complex wave fields.

To record a hologram grating, two coherent monochromatic plane waves are used, and the hologram structure represents a grating formed by some recording medium parameter, its change being due to spatial variations of the radiation intensity in the IP under recording (Fig. 1a, b).

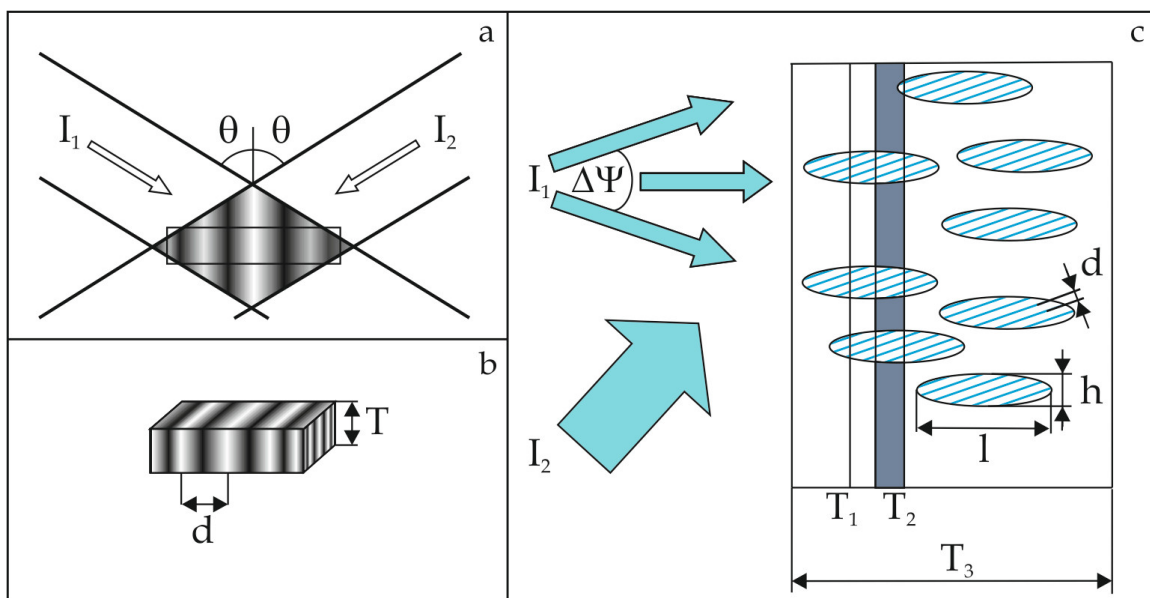


Figure 1. a, b – recording process and structure of hologram gratings: a – formation of interference pattern by interaction of two plane waves I_1 and I_2 ; b – hologram grating, where the spatial distribution of the light field intensity was transformed into variation of the absorption index of the recording medium (T is the hologram thickness, d is the IP period, 2θ is the angle between interfering beams); c – recording of holograms of complex wave fields: I_1 is the object wave with the angular spectrum half-width $\Delta\Psi$; I_2 is the reference plane wave; d is the characteristic period of the cross-modulation structure; l , h is the characteristic speckle dimensions; T_1 , T_2 , T_3 , is the recording medium thickness corresponding to different types of hologram.

A hologram grating is described with certain value of IP period, d , (or spatial frequency, $\nu = 1/d$), IP orientation with respect to recording medium boundaries, magnitude, localization, and spatial distribution of the hologram modulation amplitude. A hologram grating is the simplest hologram type, useful for practical applications. Such parameters as spatial resolution of the recording material, amplitude of modulation of optical constants in a hologram can be found exactly only for hologram gratings with certain period (spatial frequency).

The coupled wave theory describes the properties of hologram gratings (Kogelnik, 1969), which enables estimation of hologram parameters taking into account of properties of an actual recording medium.

The relationship between the period of optical parameter variation in a hologram (d) and the hologram thickness (T) determines the hologram type that is connected with important hologram properties – selectivity and the number of diffractive orders. At $T/d \rightarrow 0$, a hologram regarded as two-dimensional, at $T/d \rightarrow \infty$ – three-dimensional. As a theoretical criterion of degree of dimensionality, holography uses Klein's parameter $Q = 2\pi\lambda T/(nd^2)$ (Kogelnik, 1969), where λ is the radiation wavelength, T is the hologram thickness, n is the average refractive index of a hologram, d is the spatial period of a hologram. Klein's parameter is applicable only to describe hologram gratings that are classified as follows:

- two-dimensional, 2D, thin gratings: $Q \ll 1$.
- three-dimensional, volume gratings: $Q > 10$.

When complex wave fields composed by superposition of a set of plane components is used to record holograms, the hologram structure becomes more complicated and contains cross-modulation and intermodulation structures. Hologram cross-modulation structure is generated by interference of object and reference waves. In contrast, the intermodulation structure is generated by mutual interference of plane components of either the object wave or reference wave.

Fig. 1c shows schematically the hologram structure at interaction of a complex wave field (object wave, I_1) and a plane reference wave (I_2). The object wave has a bounded angular spectrum, $\Delta\psi$. In this case, the interference pattern generated by a set of the plane components of the object wave forms a speckle pattern (speckles are illuminated areas separated by dark regions). The speckle shape is elongated in the direction of the wave propagation (see Fig. 1c), since a speckle is $l \sim 1/(\Delta\psi)^2$ long and $h \sim 1/\Delta\psi$ wide. The hologram cross-modulation structure in the case can be schematically represented with isophase surfaces crossing the speckles, their section in the plane of drawing being schematically represented with lines with directions coincident with IP intensity maximums and orientated along the bisectrix of the angle between the reference beam and the central direction of the object beam.

Depending on the thickness of the recording medium, one can distinguish the following three hologram types as to the degree of dimensionality and use the corresponding analytical description to examine their properties.

1. 2D hologram (thin hologram): thickness of the medium (T_1) is substantially less than the characteristic dimensions of elements of hologram cross-modulation and intermodulation structures ($T_1 \ll d, l, h$). Theory – Fresnel-Kirchhoff Integral.
2. Thick film (layer) hologram (Zeldovich et al., 1986): thickness of the medium (T_2) is significantly greater than the characteristic period of cross-modulation structure, but substantially less than the characteristic dimensions of hologram intermodulation structure ($d < T_2 < l, h$). Theory – Local Kogelnick's theory.
3. Volume hologram: thickness of the medium (T_3) is significantly greater than the characteristic dimensions of elements of hologram cross-modulation and intermodulation structures ($T_3 \gg d, l, h$). Theory – Mode theory (Sidorovich, 1977, 2012), Speckle-mode theory (Zeldovich et al., 1986), Spatial-frequency version (Korzinin, 1990).

The first successful attempt to analyze the properties of volume holograms of spatially non-uniform wave fields with account of mutual rescattering by structure of a hologram of space-frequency components of wave field was the mode theory, proposed by V. G. Sidorovich. The use of the mode theory methods yielded first ever quantitative interpretation of the effect of phase-conjugate reflection under stimulated scattering (Sidorovich, 1976) and gave impetus to the further advance of theoretical studies of volume holograms.

2.2. Recording media for volume holograms

The experiments on recording volume holograms require a recording medium of physical thickness that should be on order of millimeter (from tenths of mm). Providing experimental studies with recording media is one of the main problems of volume holography, since the property package exhibited by such media cannot be ensured by traditional photomaterials (Sukhanov, 1994). Beside large physical thickness, samples of such media should have high physical and mechanical performance (to ensure invariability of the hologram structure in the course of post-exposure treatment and when operated under impact of external factors); possess high spatial resolution (thousands of lines per millimeter), sufficient energy sensitivity and transparence at the operating wavelength; and secure long-term storage and nondestructive hologram reconstruction.

The first studies in the field of three-dimensional holography made use of photochromic glasses, electro-optical crystals, photochromic and photostructured polymeric compositions (see, e. g., Sukhanov, 1994). Each of the above materials had certain drawbacks and failed to possess the set of required properties. Since the very inception of holography in three-dimensional media (Denisyuk, 1962, 1963), research and development in the field never ceased, yet there is a short line of recording medium samples for recording of volume holograms; they are manufactured in laboratory conditions, as a rule, in single pieces (or small batches) and exhibit no stable and reproducible characteristics.

It is rather difficult to present all works attempting to create recording media for volume holography with a broad spectrum of necessary parameters. The main tendencies in the development of such media were manifested most clearly in the activity of the S.I. Vavilov State Optical Institute, Russia, its staff contributing greatly to development of volume light-

sensitive media and elaboration of principles for their design (Sukhanov, 1994, 2007). The more recent of the quoted works presents the results of many years' study in the field, describes the mechanisms of hologram formation in new and original materials (their parameters are given in Table 1, reproduced from the work Sukhanov, 2007). The development of materials listed in Table 1 drew on various substances and mechanisms to create a light-sensitive composition and silicate glasses, crystals and polymeric matrices as the rigid framework. These are the directions that are actively used today.

Materials in Table 1 found their application in creation of HOE, mostly narrowband radiation selectors. Reoxan-based volume reflection hologram was used as a spectral selector (Sukhanov et al., 1984). The diffusion-enhanced medium PQ+PMMA served as a base to develop its modifications by different work groups (e. g., Steckman et al., 1998; Lin et al., 2000; Shelby, 2002; Hsu et al., 2003; Luo et al., 2008; Liu et al., 2010; Yu et al., 2010). Media on porous glass base offer great opportunities in formation of volume holograms and control of their characteristics (Sukhanov et al., 1992), but they are yet to find their application in practice because of complicated technological modes of sample production and parameter control. By virtue of their properties, identical to those of standard glass (K8, Russia), photo-thermo-refractive glass shows promise in creation of high-precision hologram elements (Efimov et al., 2004; Zlatov et al., 2010). The holographic medium on the base of CaF₂ crystals, doped with alkali metals, features high mechanical and radiation stability and damage threshold (Shcheulin et al., 2007) and shows promise in metrological applications. The samples of the material have been the base of optical element "Holographic prism" (Angervaks et al., 2010, 2012).

Characteristic	Polymeric materials		Silicate glass based		Crystal
	Reoxan (PMMA)	PQ+PMMA	Porous Glass	PTR Glass	CaF ₂
Spectral sensitivity region	440 ÷ 900	480 ÷ 540	440 ÷ 520	280 ÷ 350	300 ÷ 400
Light sensitivity, J/cm ²	0.5 ÷ 1.5	0.5 ÷ 1.5	0.01 ÷ 1	0.05 ÷ 1	≈1
Maximum value of Δn	2•10 ⁻²	5•10 ⁻³	0.1	5•10 ⁻⁴	5•10 ⁻⁵
Operating spectral range	Visible, near IR		Long-wave visible, IR		
Hologram thickness, mm	0.1 ÷ 1	0.1 ÷ 10	0.01 ÷ 1	≈1	1 ÷ 10
Thermal stability	70 °C	(70 ÷ 100) °C	500 °C	500 °C	200 °C
Pre-exposure treatment	Oxygen saturation	Not required	Not required	Not required	Not required
Development	Not required	Thermal treatment at (50 ÷ 70) °C	Chemical development, pickling	Thermal treatment at 400 and 520 °C	Not required
Fixation	Degassing	Uniform exposure	Not required	Not required	Not required
References	Lashkov & Sukhanov, 1978	Veniaminov et al., 1991	Sukhanov, 1994	Glebov et al., 1990	Shcheulin et al. 2007

Table 1. Volume recording media, developed in State Optical Institute, and their main characteristics. PMMA – polymethylmethacrylate; PQ – phenanthrenequinone; PTR Glass – photo-thermo-refractive glass.

Note that the materials listed in Table 1 are in no competition with one another, while their diversity allows making a reasonable choice proceeding from the priority requirements to be met by a specific product.

3. Some properties of volume transmission hologram gratings

3.1. Phase transmission hologram gratings

Volume hologram gratings are of great practical interest foremost in creation of hologram optical elements (HOE) used as radiation selectors. The main hologram parameters that determine properties of such elements are diffraction efficiency (DE, defined as $S \cdot S^*$ in the coupled wave theory) and hologram selectivity, both angular and spectral (defined with mismatch parameter ξ) – see Fig. 2a. In practice, the DE is found as ratio of intensity of diffracted beam (I_d) to the sum of those of zero-order (I_0) and diffracted beams (I_d) behind the hologram: $\eta = I_d / (I_d + I_0)$, and describes the efficiency of the element operation under given experimental conditions.

The limiting values of DE for hologram gratings of different types, estimated under Bragg conditions, are given in Table 2.

Hologram type	Modulated quantity	Maximum DE, %		
		Hologram recording mode		
		linear	nonlinear	
3D	transmission	absorption index	3.7	25
		refractive index	100	100
	reflection	absorption index	7.2	60
		refractive index	100	100

Table 2. Estimated limiting values of diffraction efficiency for holograms of different types.

The data for recording of holograms in linear mode are taken from the book (Collier et al., 1971) and are well known. As shown in work (Alekseev-Popov, 1981), recording holograms in nonlinear mode enables realization of the situation that allows considerable improvement of the attainable performance of a volume amplitude hologram. The presence of nonlinear effects in recording amplitude, phase and amplitude-phase holograms has a decisive role in many practical situations, as it can markedly improve the efficiency of recorded holograms.

Of greatest practical interest are volume transmission holograms that have no absorption. The DE of such holograms is described according to the coupled wave theory by expression:

$$\eta = \sin^2 \varphi_1, \quad (1)$$

where φ_1 is the phase modulation amplitude, determined by recording conditions and recording medium parameters (for symmetrical gratings):

$$\varphi_1 = \pi n_1 T / \lambda \cos \theta. \quad (2)$$

The limiting values of diffraction efficiency of both transmission and reflection phase holograms amount to 100%. The main feature of transmission holograms as distinct from reflection ones is the oscillatory nature of dependence of DE on magnitude of phase modulation. Quantity φ_1 is an important parameter in development of technology for manufacturing optical elements and in comparative analysis of theoretical calculation results and experiment, for it relates parameters of a hologram and recording medium, (first of all, the value of modulation amplitude of refractive index, n_1).

Evaluation of φ_1 by DE measurements for transmission holograms proceeds as follows. Dependence $\eta(\varphi_1)$ being of oscillatory nature, quantity φ_1 is found by formula $\varphi_1 = k\pi \pm \arcsin \sqrt{\eta}$, where $k = 0, 1, 2, 3, \dots$; to find φ_1 by DE values uniquely is possible only for holograms with $\varphi_1 < 0.5\pi$. For high-efficiency holograms, finding φ_1 by measured DE values should involve the selectivity contour shape. The situation gives grounds to divide transmission phase holograms into so-called “weak” holograms with phase modulation less than $\varphi_1 = 0.5\pi$ and “strong” holograms, where phase modulation can substantially exceed $\varphi_1 = 0.5\pi$ (e.g., Steckman et al., 1998). Note that DE values for both “weak” and “strong” holograms can coincide and be rather high. Fig. 2 gives selectivity contours of holograms that have identical DE values: $\eta = 1$ (Fig. 2a, b) and $\eta = 0.5$ (Fig. 2c, d), but different values of the phase modulation amplitude in Bragg reconstruction.

Determination of values of φ_1 for transmission phase holograms uses in addition to the selectivity contour shape also the following factors to describe “strong” hologram gratings with a given value of coefficient k :

- the sign of the first derivative $d\eta/d\varphi_1$ of variation of function $\eta(\varphi_1)$, which describes growth or drop of DE with growing φ_1 at given section;
- the sign of the second derivative $\{d^2(I_d)/(d\theta)^2\}_{Br}$ of variation of function $I_d(\theta)$ at the point of extremum of the function under Bragg conditions, which describes the appearance of selectivity contour – whether the principal maximum is present (Fig. 2c) or not (Fig. 2d);
- the ratio of DE values, measured at different polarization of reconstructing radiation, η^{TM}/η^{TE} .

As known (Kogelnik, 1969), $\varphi_1^{TM}/\varphi_1^{TE} = \cos 2\theta$, where 2θ is the angle between the zero-order and diffracted beams (in the hologram bulk) in hologram reconstruction, therefore, depending on variation interval of φ_1 , the ratio $\arcsin(\sqrt{\eta^{TM}})/\arcsin(\sqrt{\eta^{TE}})$ can be either greater or less than unity, so the value of η^{TM}/η^{TE} can be either > 1 , or < 1 . Note that the characteristic is to be used at wide enough angles between beams, since the difference between values of η^{TM} and η^{TE} at small 2θ is small too and may fall within the limits of measurement accuracy.

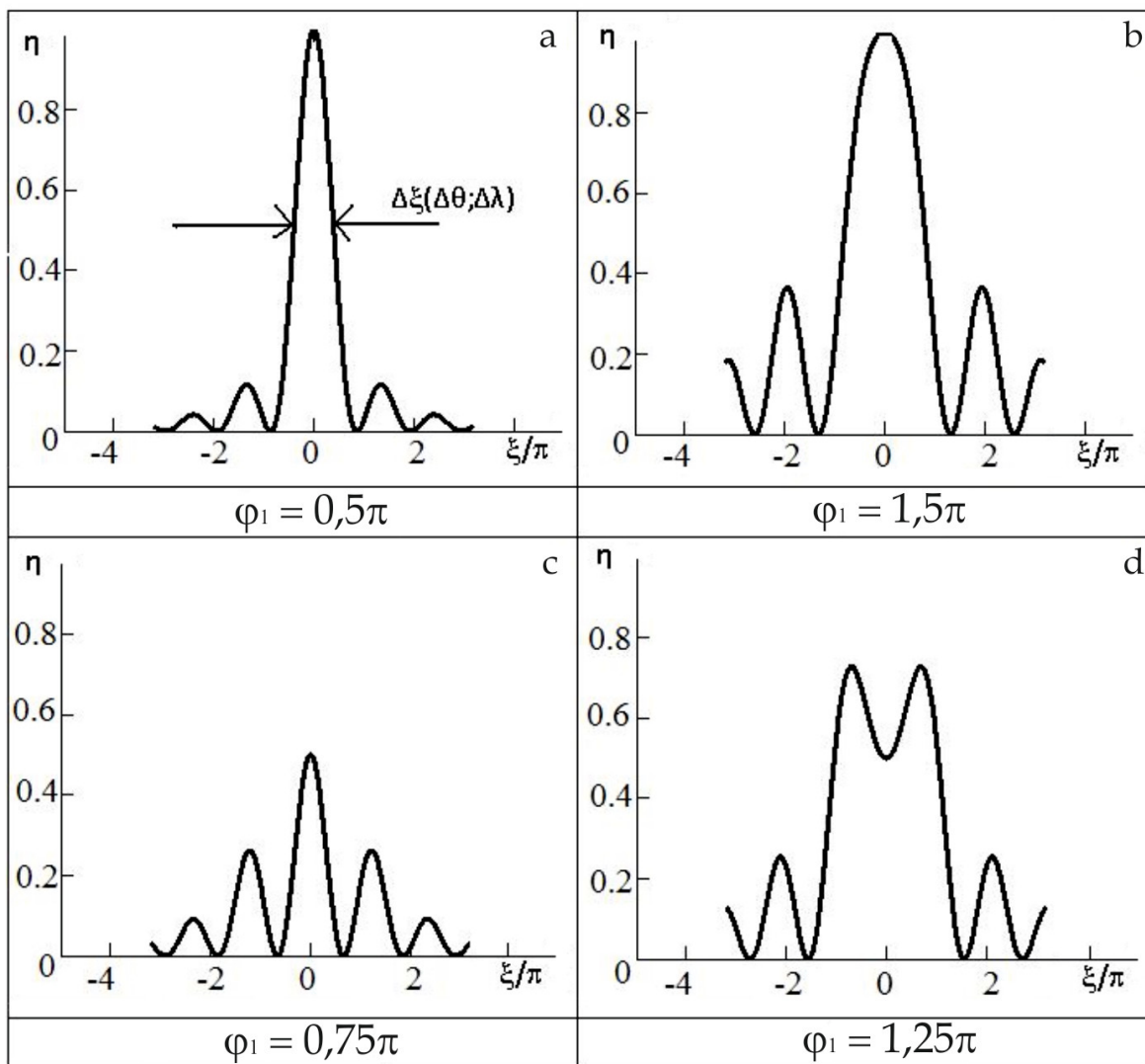


Figure 2. Selectivity contour of a volume transmission phase hologram gratings with $\eta = 1$ at $\varphi_1 = 0.5\pi$ (a) and at $\varphi_1 = 1.5\pi$ (b); with $\eta = 0.5$ at $\varphi_1 = 0.75\pi$ (c) and at $\varphi_1 = 1.25\pi$ (d). ξ is the mismatch parameter, $\Delta\xi$ is the half-width of selectivity contour of a volume hologram; $\Delta\theta$, $\Delta\lambda$ are the angular and spectral selectivity of a hologram, respectively.

Variation interval of φ_1	k	$\varphi_1(\eta)$	$d\eta/d\varphi_1$	$\{d^2(I_d)/(d\theta)^2\}_{Br}$	η^{TM}/η^{TE}
0.0 – 0.5 π	0	$\text{Arcsin}\sqrt{\eta}$	> 0	> 0	> 1
0.5 – 1.0 π	1	$\pi - \text{arcsin}\sqrt{\eta}$	< 0	> 0	< 1
1.0 – 1.5 π	2	$\pi + \text{arcsin}\sqrt{\eta}$	> 0	< 0	> 1
1.5 – 2.0 π	3	$2\pi - \text{arcsin}\sqrt{\eta}$	< 0	> 0	< 1

Table 3. Additional data for finding the value of phase modulation of transmission holograms by measured DE values and angular selectivity contour shape of a hologram.

3.2. Energy channelizing in the volume transmission phase hologram grating

Diffraction of an intensity-uniform monochromatic plane wave by a volume hologram grating structure finds an adequate description in the coupled wave theory (Kogelnik, 1969). Consider propagation of radiation in a “strong” ($\varphi_1 \gg \pi/2$) transmission phase hologram grating, recorded symmetrically, under Bragg incidence of reconstruction radiation as shown in Fig. 3.

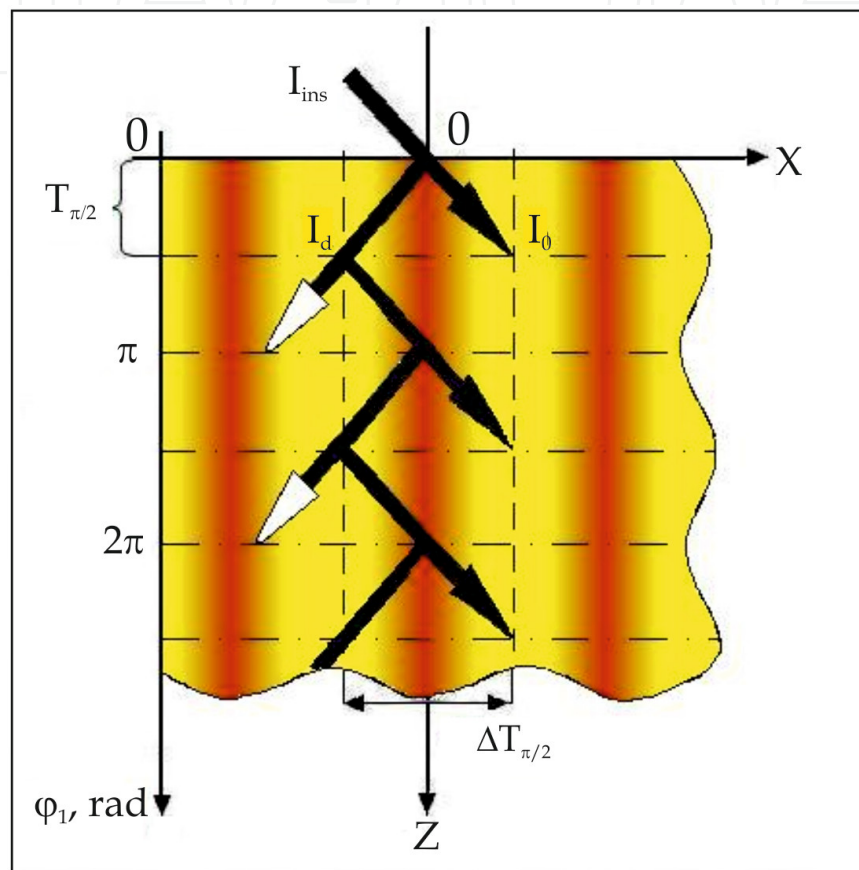


Figure 3. Process of radiation propagation in a “strong” transmission phase hologram grating, recorded symmetrically, under Bragg incidence reconstruction radiation: dot-and-dash lines are hologram planes that correspond to the values $\varphi_1 = k\pi/2$, where $k = 1, 2, 3, \dots$; $\Delta x_{\pi/2}$ is the cross-section of the channel of radiation energy propagation; $T_{\pi/2}$ is the thickness of hologram layer with $\varphi_1 = \pi/2$.

Of special importance during reconstruction of a “strong” volume hologram grating are the hologram areas, where function $\eta(\varphi_1)$ has extremums (in Fig. 3 the extremum planes appear as dot-and-dash lines) – these are the hologram planes that correspond to the values of phase modulation amplitude of diffracted radiation, $\varphi_1 = k\pi/2$, where $k = 1, 2, 3, \dots$. In accordance with the concepts of the coupled wave theory, the vector of the radiation propagation in a hologram changes its direction in each extremum plane of function $\eta(\varphi_1)$. The geometrical dimensions of the radiation propagation channel in a hologram are clearly seen to be bounded and less than size $\Delta x_{\pi/2}$, as shown on the diagram in Fig. 3: $\Delta x_{\pi/2}$ is found in extremum plane of function $\eta(\varphi_1)$ with $k = 1$, where $\varphi_1 = \pi/2$; the thickness of the hologram layer is denoted as $T_{\pi/2}$.

Thus, under Bragg incidence of a reconstructing beam at the entrance face of hologram grating, the propagation of the energy of diffracted and zero-order beams occurs along isophase hologram planes, i. e. radiation energy is channelized and the geometrical cross-section of its propagation channel is bounded by value $\Delta x_{\pi/2}$.

As shown by the present author's theoretical calculations, the effect of energy channelizing by "strong" transmission hologram gratings is exhibited also in the diffraction of reconstruction radiation with nonuniform intensity distribution, as it occurs in case of actual light beams. Besides, within the framework of the coupled wave theory, the energy channelizing effect has been shown to reveal itself at its fullest in case of angular spectrum ($\Delta\psi$) of the incident monochromatic wave being much narrower than the width of the angular selectivity contour of a hologram layer of thickness $T_{\pi/2}$, which is equivalent to the requirement of the beam diameter (or its size in the section plane of the hologram considered in Fig. 3) being much greater than the thickness of the hologram layer ($T_{\pi/2}$), where $\varphi_1 = \pi/2$.

The author's experiments in 2008, reported at "Holoexpo-2008" conference, confirmed the manifestation of the energy channelizing effect when reconstructing beam of radiation with nonuniform intensity distribution is used. The experiments involved PTR-glass samples 9 mm thick, where hologram gratings were recorded under symmetrical incidence of interfering beams onto sample surface at a 45-degree angle. Interference planes in a hologram were situated perpendicularly to the front and rear sample surfaces, as shown in Fig. 4a, b. The hologram recording conditions allowed setting the recording regime, needed to obtain a hologram grating with the required value of phase modulation amplitude.

The value of phase modulation amplitude was in one case as low as $\varphi_1 \approx 0.25\pi$ (Fig.4a, c – "weak" hologram, as $\varphi_1 < \pi/2$) and in another as high as $\varphi_1 = 10.25\pi$ (Fig.4 b, d – "strong" hologram). Fig. 4 presents the schematic view (a, b) of radiation propagations as well as the radiation energy distribution (c, d) on the front and rear faces of studied samples of identical thickness. The photograph in Fig. 5 a fixates the process of reconstruction of a "strong" hologram (the date are given in Fig. 4 b, d): one can clearly see the energy propagation channel, orientated perpendicularly to the front and rear sample faces, i. e. directed along the isophase surfaces of the hologram.

The energy distributions in radiation beams on the hologram entrance and exit faces (Fig. 4 c, d) are processed experimental results. Parameters of beams on the hologram entrance face correspond to those of reconstructing beams used in the experiment, while the beam intensity distribution on the exit hologram face is calculated with account of the hologram phase modulation. The phase modulation for each hologram was found experimentally by the DE value and the shape of the angular selectivity contour. The calculation for Bragg diffraction of Gaussian beams by periodically modulated media used the technique, published in works (Chu & Tamir, 1976). The calculated results for the beam intensity distribution on the exit hologram face are in qualitative agreement with the picture of beam diffraction, observed in the experiment.

As noted, the terms “weak” hologram and “strong” hologram for a transmission volume phase hologram bear no relation to the DE value, but are defined by the value of phase modulation amplitude φ_1 . The DE value for holograms in the experiment, which was attained under Bragg conditions in the two cases is less than 50% for both the “weak” and the “strong” holograms. Despite the close values of DE, the appearance of the spatial intensity distribution for either of the two interacting beams (diffracted and zero-order ones) on the hologram exit face differs markedly. As seen from the data of Fig. 4 a, c, intensity distribution of diffracted and zero-order beams on the exit face of a “weak” hologram 9 mm thick exhibits two peaks that are spaced apart and correspond to the diffracted beam and zero-order diffraction beam (transmitted one). Here, the diffracted beam is appreciably broadened with respect to the incident one and exits the hologram strictly opposite to the incident one, i. e. the diffracted beam energy propagates along antinodes of a hologram grating, which is schematically illustrated in Fig. 4 a. The zero-order diffraction beam propagates practically in the direction, prescribed by ray optics.

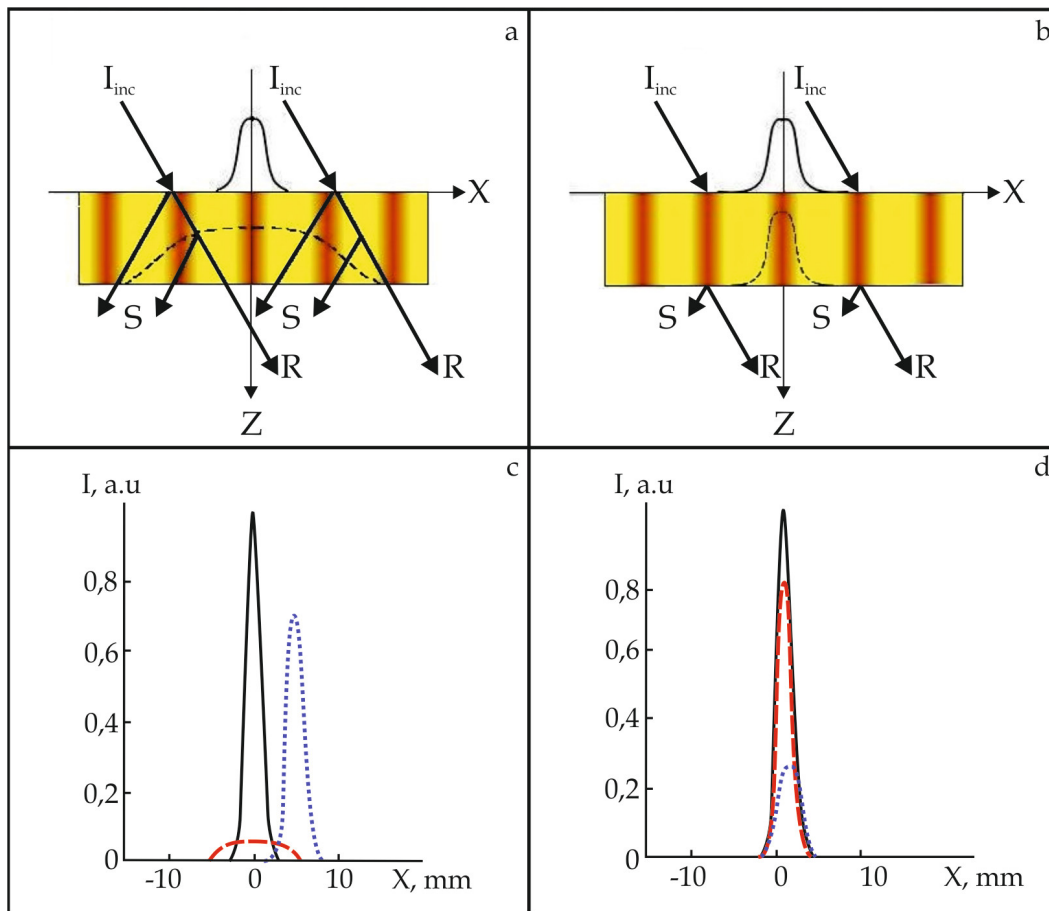


Figure 4. Reconstruction of symmetrically-recorded hologram gratings in samples of identical thickness ($T = 9$ mm): “weak” hologram with $\varphi_1 \approx 0.25\pi$ (a, c) and “strong” hologram with $\varphi_1 = 10.25\pi$ (b, d); a, b - radiation propagation diagram, where I_{inc} is the incident (reconstructing) beam, S is the diffracted beam, R is the zero-order diffraction beam; c, d - radiation intensity distribution in the reconstructing beam on the entrance hologram face (solid curves), and in zero-order (dot lines) and diffracted (dash lines) beams at the hologram exit face.

On the exit surface of a “strong” hologram, however:

- the diffracted beam and zero-order diffraction beam are spatially aligned with each other;
- the intensity distribution in zero-order and diffracted beams is practically no different from that in the reconstructing radiation beam;
- the spatial position of the beams specifies the direction of isophase surfaces, along which the radiation propagates.

Reconstruction radiation parameters			Hologram parameters				Channelizing conditions		
Beam D, mm	$\Delta\psi$, mrad	Incid. angle	T, mm	φ_1 , rad	$T_{\pi/2}$, mm	$\Delta\theta$, mrad	$\frac{\Delta\psi}{\Delta\theta}$	$D/T_{\pi/2}$	$\Delta x_{\pi/2}$, mm
3	0.3	θ_{Br}	9	10.25π	0.45	> 3	< 0.1	> 7	4

Table 4. The conditions for running the experiment to observe the energy channelizing effect in reconstruction of a hologram grating 9 mm thick.

Table 4 shows hologram grating parameters that enable the observation of the energy channelizing effect.

Special notice should be given to the situation observed in the reconstruction of a “strong” hologram beyond Bragg angle. Fig. 5 b shows dependences, obtained in non-Bragg reconstruction of the “strong” hologram, its reconstruction results at Bragg angle having been given in Fig. 4 d. The deviation from Bragg angle in the case was 0.4 mrad, so, after crossing the entrance sample surface, the zero-order beam propagated in the hologram both within the angular selectivity contour $\Delta\theta$ of the hologram, (see Fig. 2 a) and partially outside its limits.

The data in Fig. 5 b demonstrate a very interesting situation: the channelized radiation intensity in the direction of the isophase surfaces is zero as distinct from Bragg conditions of reconstruction, whereas another two radiation propagation channels emerge symmetrically to the right and the left with respect to the “Bragg” propagation channel.

What is the possible reason behind the emergence of two radiation propagation channels? One can suggest the following general behavior of propagating beams in a volume hologram grating in non-Bragg reconstruction of the “strong” hologram. The reconstructing radiation beam deviated from Bragg reconstruction condition by value 0.4 mrad that is less than the half-width of the angular selectivity contour of a hologram at $\varphi_1 = \pi/2$, which is in the present experiment about $\Delta\theta \approx 3$ mrad. Having passed the plane of the first extremum of function $\eta(\varphi_1)$ (at $T_{\pi/2}$), this so-called “first” zero-order beam (I_{01}) can, by virtue of small deviation from Bragg angle, bifurcate and continue partially propagating in the original position, thus forming the “second” zero-order beam (I_{02}) that can likewise bifurcate after passing the hologram section T_{π} and from the “third” zero-order beam, propagating at the same angle as I_{02} symmetrically with respect to I_{01} . Each of the zero-order beams can form its “own” propagation channel that should remain, according to theoretical concepts, within the geometrical limits of the cross-sectional area $\Delta x_{\pi/2}$ of the hologram, but may be misaligned with the direction of the radiation propagation under Bragg reconstruction conditions.

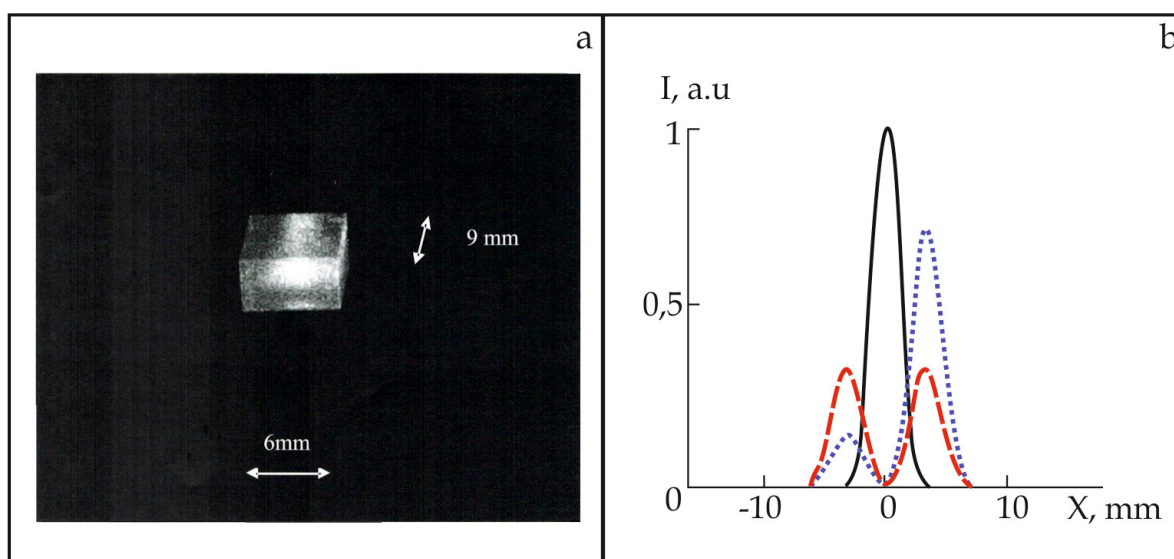


Figure 5. a - observation of the energy channelizing effect in volume hologram grating 9 mm thick with phase modulation amplitude 10.25π , recorded in PTR-glass: incident beam illuminates the sample exit face at a 45-degree angle, beam diameter is 3 mm. b - processed experimental results for reconstruction of a “strong” hologram at a deviation from Bragg angle by 0.4 mrad: radiation intensity distributions in the reconstructing beam on the hologram entrance surface (solid curves); in zero-order (dot line) and diffracted (dash line) beams on the hologram exit face. Hologram parameters are the same as given in Fig4 d and Fig. 5 a.

Thus, the present experiment has realized the scenario of “bifurcation” of radiation propagation channels by way of selection of non-Bragg reconstruction; in addition, intensity distributions of the zero-order and diffracted beams on the hologram exit surface were calculated for the case. The results of intensity distribution calculations are in qualitative agreement with the picture of beam diffraction, observed in the experiment. Theoretically, one can realize the situation with a large number of propagation channels that should theoretically lie within the limits, defined by the conditions of the experiment on observation of the energy channelizing effect (see Fig. 3.).

4. The effect of ambient conditions on volume hologram parameters

4.1. The effect of ambient variations on parameters of recording media

A recording medium to produce volume holograms should, as already mentioned, be about a millimeter thick and ensure the invariability of hologram structure in the course of treatment and operation. The temperature is one of the main ambient parameters with its effect to be allowed for when handling HOE. Temperature variation causes changes in both linear dimensions and refractive index of a sample. Table 5 lists characteristics that enable assessment the temperature-induced changes in parameters of samples of recording materials in use.

Note that the changes occurring in samples at varying ambient temperature are, as a rule, interrelated. i. e. a drop in refractive index is due to an increase in sample dimen-

sions (its expansion), while sample contraction causes the index to grow. At the same time, the processes of hologram recording and post-exposure treatment have a selective effect on sample parameters: either recording or post-exposure treatment necessarily results in a refractive index change, with the geometrical dimensions of the medium remaining practically the same (the media are then called “shrinkproof”) or undergoing slight changes (media with “negligible shrinkage”). Media on silicate glass base are commonly believed to be shrinkproof; yet when the holograms are recorded on PTR-Glass samples (see Table 1), the average refractive index changes in the course of thermal post-exposure treatment by a noticeable value $\sim 10^{-4}$ (Glebov, et al., 2002). This is to be allowed for in design of HOE with prescribed performance.

Characteristic	Material		
	Polymer	Silicate glass	Crystal, CaF ₂
Linear thermal expansion, dl/dT , K ⁻¹	$(3.6 \div 6.5) \cdot 10^{-5}$	$(5 \div 9) \cdot 10^{-6}$	$18.9 \cdot 10^{-6*}$
Refractive index, dn/dT , K ⁻¹	$-1.05 \cdot 10^{-4}$	$-(10^{-5} \div 10^{-6})$	$-8.7 \cdot 10^{-6}$
References	Marvin, 2003; * Malitson, 1963		

Table 5. The temperature effect on the changes in refractive index and dimensions of samples used to produce volume recording media

As seen from the data of Table 5, the changes in parameters of polymeric media at varying temperature are substantively (severalfold) larger than those of media on the base of silicate glass and crystals. In addition, polymers exhibit a property to take up moisture, which in turn causes changes in sample thickness and average refractive index; therefore, handling the polymeric samples makes it necessary to maintain the ambience stable.

Experiments on recording and reconstruction of holograms, produced on silicate glasses and crystals, are held under ambient conditions, maintained as a rule at the level of standard conditions of a research laboratory (temperature variation is ± 1 K, humidity variation is 3÷5%). The accuracy, within which one should maintain the ambient temperature and humidity for the conditions to be considered stable for polymeric samples, is dependent on the recording medium properties and the prescribed requirements to hologram parameters. The present section gives the results of experiments on the temperature and humidity effect on parameters of hologram gratings (1.0 ÷ 1.4) mm thick, which were produced on samples of polymeric material Difphen at recording by radiation with $c \lambda = 488$ nm at spatial frequency $\nu = (300 \div 500)$ mm⁻¹.

The results obtained for a PMMA-based polymeric recording medium can be used to optimize the conditions of experimental operation of different polymeric samples in recording and reconstruction of information.

4.2. The effect of temperature variation on parameters of polymeric volume holograms

4.2.1. The experimental technique with the use of low-frequency interference pattern

The effect of temperature on parameters of polymeric volume hologram gratings was assessed by observation of behavior of low-frequency interference pattern (IP). The schematic diagram of the experiment is given in Fig. 6. It was carried out with the use of a stand intended for hologram recording, the same where the hologram under study was recorded.

Hologram grating was mounted into the scheme in the position it had had during recording and illuminated by two coherent beams I_1 and I_2 . Each of the incident beams was diffracted by the hologram structure with formation of its “own” diffracted beam: beam I_1 formed diffracted beam I_{1d} that propagated in the same direction as beam I_{20} , and beam I_2 formed diffracted beam I_{2d} that propagated in the same direction as beam I_{10} . When the hologram was shifted, an angle, 2φ , was formed between beams that propagated behind the hologram in the same direction (I_{1d} and I_{20} ; I_{2d} and I_{10}), and the IP was formed in the space where the beams superimposed. At a turn of the hologram through angle $\varphi = 0.1$ mrad, the pattern period, d , has according to Bragg condition the value $d \approx 2.5$ mm.

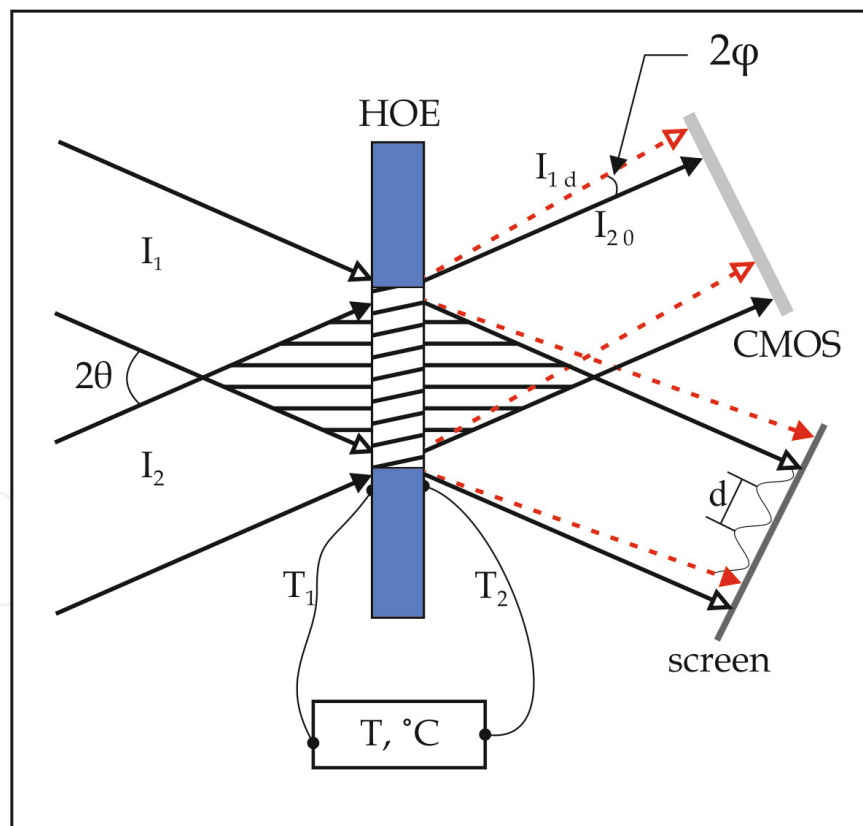


Figure 6. Diagram of the experiment on creation of low-frequency interference pattern: I_1 and I_2 are coherent beams of collimated radiation with $\lambda = 488$ nm; 2θ is the angle between beams I_1 and I_2 in the air; HOE is the hologram grating; T_1 and T_2 are temperature sensors; I_{1d} , I_{2d} , I_{10} , I_{20} are beams of radiation diffracted by a hologram grating (first and zero orders); 2φ is the angle between beams that form the low-frequency IP.

The forming interference pattern can be observed in each of propagating beams (I_1 and I_2) with a screen installed perpendicularly to the beam propagation. The IP was recorded using a CMOS matrix of a size that allowed recording the observed interference field in full and obtaining interferograms imaged in Fig.7a, b. The interferograms were shot at actual size simultaneously with temperature control. The temperature sensors, mounted onto the sample on the side 1 (T_1) and on the side 2 (T_2) in close proximity to the observation area, allowed carrying out the control with accuracy 0.1 K.

Before the experiment started, the hologram was set in the position, where the IP had the maximum period that provided the possibility under those conditions to process interferograms and perform quantitative measurements. To measure the temperature, a warm air jet was directed towards the hologram on the side 2 and the sample was heated up to temperature $T = 32$ °C. The interferograms were shot in a stationary state of the scheme, with the sample cooling down after the action of warm air; the difference in readings T_1 and T_2 was within the measurements accuracy.

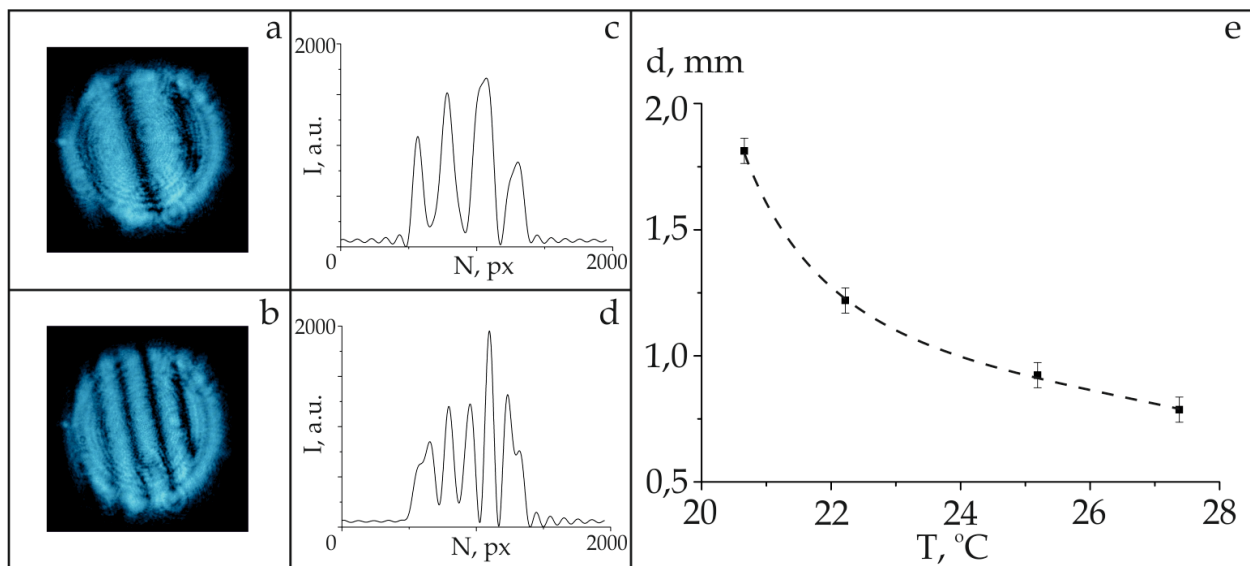


Figure 7. Changes of the period of the low-frequency interference pattern (IP) at variation of the temperature of polymeric hologram grating with $\nu = 350 \text{ mm}^{-1}$, recorded on a sample of Difphen material 1.2 mm thick: a, b – IP images at hologram temperature 21 °C (a) and 27 °C (b); c, d – processing of interferograms given in a and b, respectively; e – dependence of IP period, d, on sample temperature, dashed line illustrate the character of process.

4.2.2. The experimental results

The experiment was carried out under the following conditions: interfering beam diameter, D , 8–10 mm; angle between beams I_1 and I_2 , 2θ , 10 deg.; $\lambda = 488 \text{ nm}$; angular selectivity of the hologram under study, $\Delta\theta$, 1.7 mrad; temperature variation interval 21–28 °C.

The obtained interferograms and the results of their processing are given in Fig. 7 a-d. The dependence of IP period change on sample temperature is given in Fig. 7 e. As seen, with the temperature growing from 21 to 28 deg., the IP period changed from 1.8 mm to 0.7 mm, which corresponds to a change in angle 2φ (θ_{\max} shift) by 0.43 mrad. The experiment showed no change (within the measurements accuracy) in the IP period, measured before the start of measurements and after the sample cooled down to the room temperature. Thus, one can estimate the effect of temperature variation on parameters of polymeric hologram 1.2 mm thick with spatial frequency $\nu = 350 \text{ mm}^{-1}$ as follows: with the temperature changing by 1K, the change in the diffraction angle (θ_{\max} shift) amounts to $\delta\theta_{\max} = 0.06 \text{ mrad}$, i. e. the hologram under study has thermal shift 0.06 mrad/K.

Note that the temperature effect on parameters of polymeric reflection holograms, recorded on samples of Reoxan material (Sukhanov et al., 1984), demonstrates the magnitude of changes on the same order. With the temperature of Reoxan sample changing from 24 °C to 29 °C, the shift of λ_{\max} in the spectrum of reflected radiation is from 532.1 nm to 532.6 nm (spectral interval of reconstructing radiation, $\Delta\lambda < 0.01 \text{ nm}$). Thus, the studied hologram (thickness 1 mm, $\nu > 3000 \text{ mm}^{-1}$, spectral selectivity, $\Delta\lambda = 0.15 \text{ nm}$), intended for the use as a narrowband spectral selector, had thermal shift $\delta\lambda_{\max} = 0.1 \text{ nm/K}$.

4.3. The effect of ambient humidity variation on parameters of polymeric volume holograms

4.3.1. The method of assessment of the change in the space position of diffracted beam

It has been established that a Difphen material sample (a disk 40 mm in diameter and 4 mm thick), when immersed in water in the temperature range (20 ÷ 30) °C, takes up to 1.5% of water with respect to the sample weight in air-dry condition at relative humidity of the ambient air $H \approx 50\%$. Taking up moisture changes the average refractive index and thickness of the sample and, accordingly, characteristics of recorded holograms.

The effect of varying humidity of the ambient air on the polymeric hologram parameters was studied at an experimental stand of a design that provided for an enclosed volume around the hologram to maintain humidity $\approx 90\%$ (much higher than normal conditions) and for conduct of long-time measurements (several hours). Fig. 8 shows the optical diagram of the stand (Fig. 8 a) and schematic drawing to illustrate possible changes in polymeric sample dimensions under moisture take-up (Fig. 8 b).

The stand was used to measure the angular selectivity contour of a hologram at a one-time fixation of all contour data. The hologram was illuminated with a divergent radiation beam; the intensity distribution of the diffracted radiation (angular selectivity contour) was recorded by a CMOS matrix of a camera – the results of processing the experimental data are given in Fig. 9. The effect of varying humidity on hologram parameters was assessed by a change in the position, θ_{\max} , of the intensity maximum of diffracted radiation in a CMOS matrix during the process under study. Position θ_{\max} was detected with accuracy ± 1 pixel, which corresponded to angular resolution $\approx 0.02 \text{ mrad}$.

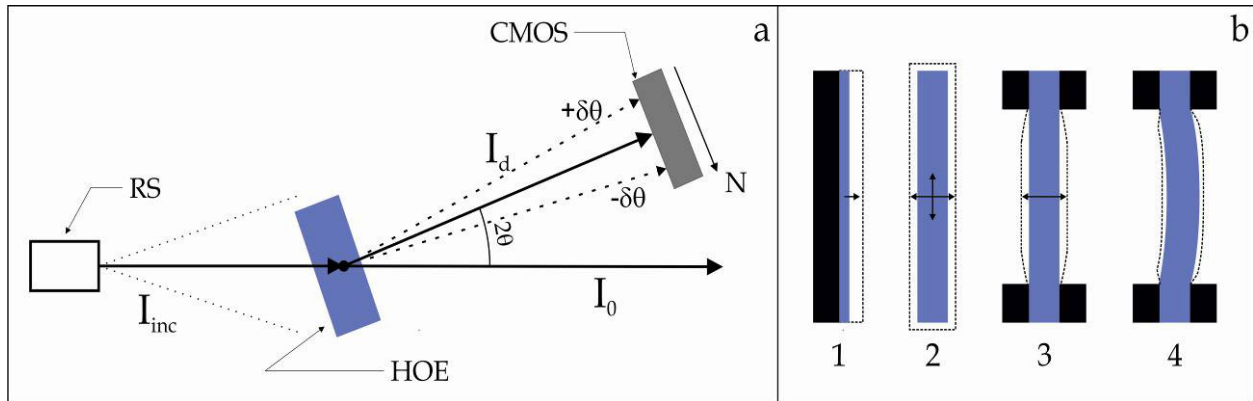


Figure 8. a – optical diagram of experiment to assess the changes of hologram parameters under varying ambient humidity: RS – radiation source, I_{inc} is the incident (reconstructing) beam, I_d is the diffracted beam, I_0 is the zero-order diffraction beam, 2θ is the diffraction angle, $\pm\delta\theta$ is the diffraction angle change, N is the readout of pixel number in CMOS matrix (in the arrow direction). b – polymeric sample growing in size upon taking up moisture: 1 – the sample is fixed in a rigid framework, 2 – the sample is in free state, 3, 4 – the sample is fixed in a cartridge, geometrical dimensions of a sample upon taking up moisture are dash lines, arrows show the size growth direction.

4.3.2. The experimental results

The experimental results are presented in Fig.9. Fig. 9 a shows the position θ_{max} of a hologram at ambient humidity 40% and 90%. A change of position θ_{max} in the present experiment corresponded to the increase of the diffraction angle and was as large as $\delta\theta_{max} \approx +0.25$ mrad. It is this value that characterizes the difference in hologram parameters in two stable states of the sample at different humidity.

The process of hologram relaxation (stabilization of its parameters) at a sudden drop of the ambient humidity from 85% to 50% is illustrated by Fig. 9 b. The stabilization of hologram parameters in changed conditions was accompanied by a change in the position of the selectivity contour maximum, which corresponds to a decrease of the diffraction angle and a shift of θ_{max} by $\delta\theta_{max} \approx (0.10-0.18)$ mrad, fixed in 2.5 hours after the sudden variation of the humidity. As shown by results of experiments on different samples, position θ_{max} at a sudden drop of the ambient humidity from (85 ÷ 90)% to (40 ÷ 50)%, attains its steady state value, which remains later practically the same, in 2-3 hours (relaxation time is dependent on sample properties), while θ_{max} shifts by $\delta\theta_{max} < 0.3$ mrad.

Thus, one can estimate the change in the diffraction angle at humidity change of 5% (which accords with typical excursions of workroom humidity) to be $(\delta\theta_{max})_{5\%} < 0.03$ mrad and recommend to keep a polymeric hologram in stable conditions for at least two-three hours for stabilization of its internal structure. The effect of changing ambient temperature and humidity on the parameters of polymeric hologram gratings is given in Table 6.

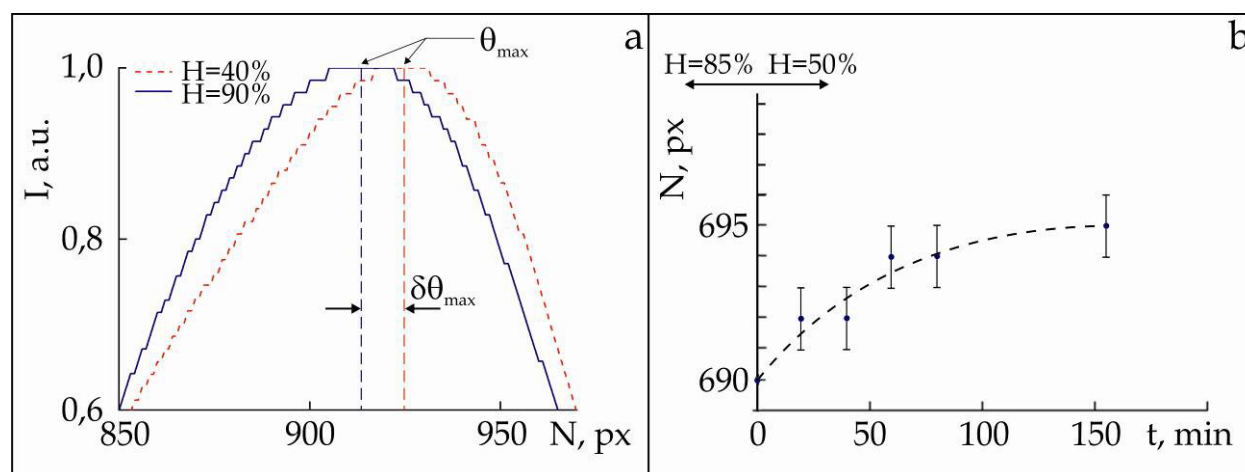


Figure 9. Processing of experimental results: a – the position of the angular selectivity contour maximum, θ_{\max} , in CMOS matrix at ambient humidity $H \approx 40\%$ (dot line) and $H \approx 90\%$ (solid line), $\delta\theta_{\max}$ is the position θ_{\max} shift (hologram with $\nu \approx 450 \text{ mm}^{-1}$); b – the relaxation of hologram grating at a sudden change in humidity from 85% to 50% (hologram with $\nu \approx 350 \text{ mm}^{-1}$), dashed line illustrate the character of process.

It shall be remembered that the recording of holograms under study took place, as a rule, at the ambient humidity $H \approx (50 \div 60)\%$. With rising humidity, the growing of dimensions of a sample, rigidly fixed in a cartridge (Fig. 8 b, positions 3, 4), is accompanied by some deformation unlike the sample in a rigid framework and that in a free state (Fig. 8 b, positions 1 and 2, respectively). The sample, fixed in a rigid framework is as a rule a film one in silicate glass framework. When such sample takes up moisture, only the change in its thickness is considered (as, e. g., in the work Pandey et al., 2008). Here, side 1 of the sample is rigidly with the framework and never changes its position in space.

Ambience variation		Hologram parameter variation		
Property	Amount of change	Parameter	Amount of change	Recording material
Humidity, rel. %	5%	θ_{\max} shift	0.03 mrad	Difphen, $\nu \approx 450 \text{ mm}^{-1}$
Temperature, K	1 K	θ_{\max} shift	0.06 mrad	Difphen, $\nu \approx 350 \text{ mm}^{-1}$
		λ_{\max} shift	0.1 nm	Reoxan $\nu > 3000 \text{ mm}^{-1}$

Table 6. The effect of variation of ambient temperature and humidity on the parameters of polymeric volume hologram gratings about 1 mm thick.

The sample in a free state grows in size, when taking up moisture, along all three coordinates. The sample, rigidly fixed in a cartridge (Fig. 8 b, positions 3, 4), grows in volume, when taking up moisture, due to increasing thickness, with position of sides 1 and 2 of the sample changing relative to its center. At lesser deformations, the position of the sample center in space remains the same (Fig. 8 b, position 3). Yet, if the sample volume growth exceeds the threshold deformation values determined by the sample geometry (the ratio of diameter to thickness), the performed calculations have revealed the possibility of the sample bending and the sample center shifting in space, as shown in Fig. 8 b, position 4.

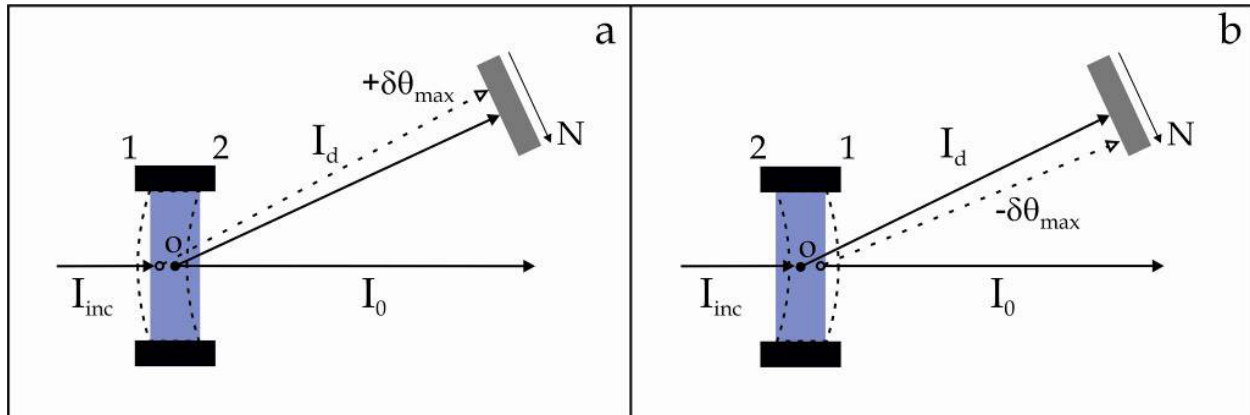


Figure 10. Diagram of experiment on observation of shifts of the diffracted beam (I_d) during hologram reconstruction from side 1 (a) and side 2 (b) - deformation with a shift along the sample axis. I_{inc} is the incident (reconstruction) beam; I_0 is the zero-order diffraction beam; O is the sample center without deformations; 1 and 2 are the sample sides; N is the CMOS matrix (the pixel number is counted in the arrow direction).

The presence of sample deformations due to its bending at taking-up the moisture has been detected in experiments on observation of the shift of the diffracted beam during reconstruction of a hologram from either sample side. The experiment diagram is given in Fig. 10. Its implementation contains five stages. Fig. 11 gives the results of processing of the performed experiment and shows the change in position θ_{max} in CMOS matrix at stages 1, 3, 5. Stage 1: the sample in steady state is mounted in a cartridge (at workroom humidity $H \approx 50\%$), and angular selectivity contours are shot for several scores of minutes (Fig.11 – stage 1). Stage 2: enclosed volume is established around the sample (HOE) using a protective housing, where humidity $H \approx 90\%$ is maintained, the stage duration is about 20 hours. Stage 3: protective housing is removed, and selectivity contours are shot in automatic mode under hologram relaxation in conditions of workroom humidity (Fig. 11 – stage 3). Stage 4: the sample is kept in stable workroom conditions for about 20 hours. Stage 5: angular selectivity contours are shot for a hologram in steady state.

As seen from experimental data of Fig.11, position θ_{max} in steady state of the hologram (stages 1 and 5) is stable and lies within measurement accuracy during reconstruction from both side 1 and side 2. However, position θ_{max} at $H \approx 90\%$ (value N at $t = 0$ at stage 3) as compared to that at $H \approx (40 \div 60)\%$ demonstrates growth of the diffraction angle during hologram reconstruction from side 1 and decrease of the diffraction angle during reconstruction from side 2. Such situation may be due to the presence of sample deformations with a shift of its center in space (sample bending), as shown schematically on Fig. 10 a, b.

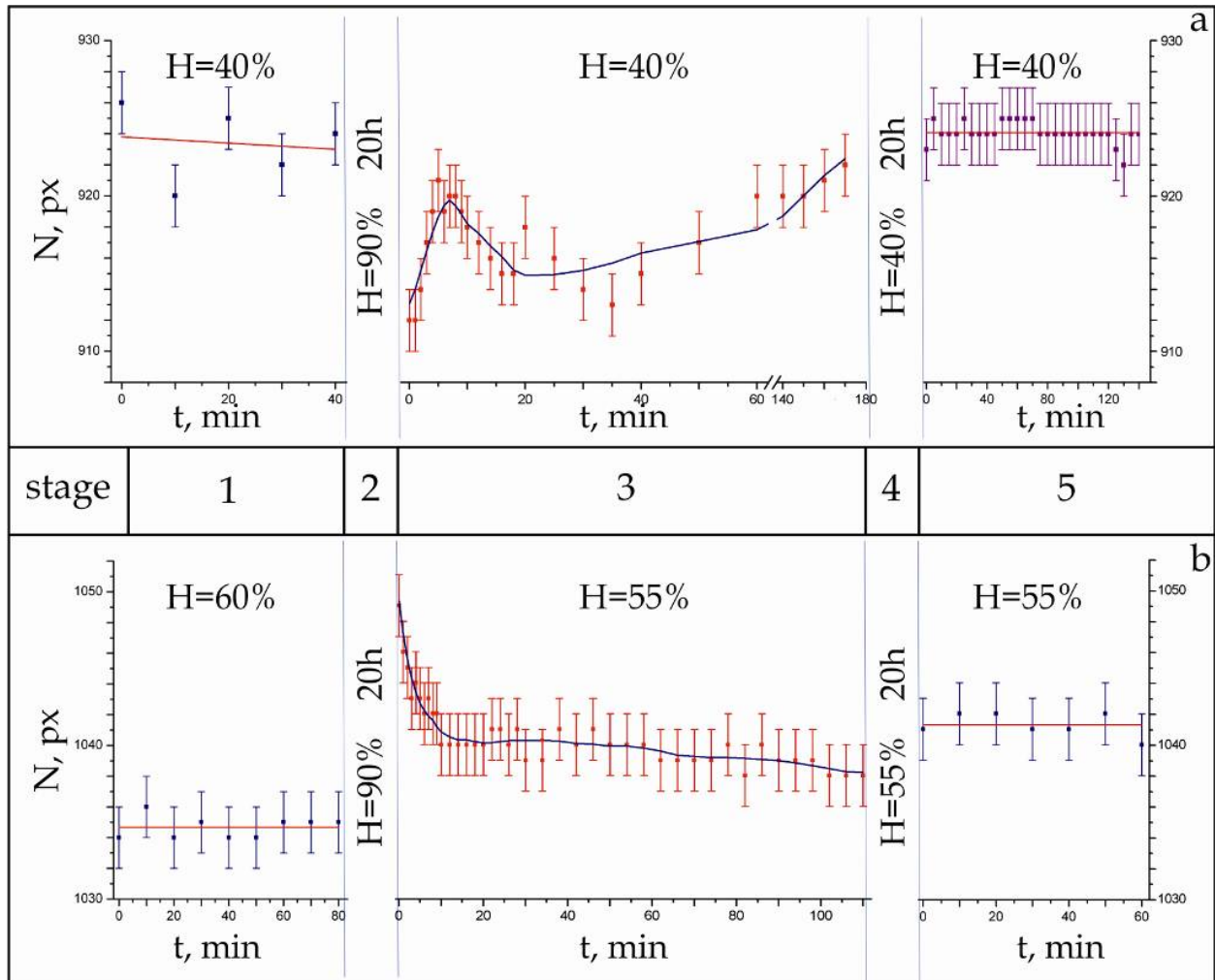


Figure 11. Results of experiment on observation of shifts of θ_{\max} during hologram reconstruction from side 1 (a) and side 2 (b): plots show the pixel number in CMOS matrix, N , corresponding to position θ_{\max} of a hologram at given instant of time in steady state (stages 1, 5) and out of the critical deformation (stage 3). Hologram with $v \approx 450 \text{ mm}^{-1}$.

5. Conclusion

The present work discusses properties and specific features of volume holograms as well as results of original experiments that demonstrate unique potentiality of such holograms.

The results of examination of parameters are given for phase volume transmission hologram gratings that are of practical importance, and the hologram features are discussed, which are related to radiation propagation in media of great thickness with periodic structure on the

order of the radiation wavelength. Practical recommendations are given to allow finding the phase modulation amplitude of “strong” hologram gratings by the value of diffraction efficiency and the shape of selectivity contour.

Experimental results are presented, which prove the existence of the effect of energy channelizing by “strong” transmission hologram gratings when using a reconstruction radiation beam with non-uniform intensity distribution, and the experimental conditions are defined for the effect to be revealed. The energy propagation in such structures has been shown to be confined to area occupied by the interacting beams (zero-order and diffracted) upon attaining $\varphi_1 = 0.5\pi$, the first extremum of function $\eta(\varphi_1)$. An effect was found of beam bifurcation and emergence of two channels for radiation propagation during reconstruction of a “strong” hologram grating beyond Bragg angle.

Parameters are listed for recording media to produce volume holograms, they were developed according to principles of recording media design, proposed in late 80s of the last century by S.I. Vavilov State Optical Institute specialists. The information is still topical as the last two decades saw mostly refinement, modification, and improvement of variants of volume recording media manufactured in laboratory conditions.

The effect of ambient temperature and humidity was studied for parameters of polymeric hologram gratings about 1 mm thick with spatial frequency $\sim (350 \div 450) \text{ mm}^{-1}$, which were produced on Difphen material samples. The results allow estimating the change in the diffraction angle as $\approx 0.06 \text{ mrad}$ at temperature variation by 1°K and as $\approx 0.03 \text{ mrad}$ at relative humidity variation 5%. Despite the dependence of the values on the sample physical and mechanical properties, geometry and history, the estimates can be used to plan the working conditions for HOE on base of different polymers and to optimize the experimental conditions for handling polymer samples in information recording and reconstruction.

Experimental data were obtained to substantiate the assumption that taking-up of moisture can result not only in a change in thickness of a sample, rigidly fixed in a cartridge spatial, but also in its deformation, describable as “bending”. Bending-type deformation was observed in conditions of high humidity on a sample with the diameter/thickness ratio of about 40:1. Thus, hologram gratings can be used to study deformation of materials under impact of ambient conditions.

The study of the temperature effect on parameters of polymeric hologram gratings employed an original technique for observing hologram deformations with the help of low-frequency interference pattern. The obtained results demonstrated efficiency of the technique and high accuracy of detecting the changes of hologram parameters.

Acknowledgements

The authors express their gratitude for participation in the experiments and assistance in preparation of the publication to A.A. Paramonov, S.A. Chivilikhin, D.A. Gomon, O.V. Bandyuk, V.V. Lesnichy, A.S. Zlatov, P.A. Kudriavcev.

Author details

O.V. Andreeva, Yu.L. Korzinin and B.G. Manukhin

The National Research University of Information Technologies, Mechanics and Optics, Russia

References

- [1] Alekseev-Popov, A.V. (1981). *J. Technical Physics*, Vol.51(6), pp. 1275-1278, USSR
- [2] Angervaks, A.E. et al (2010, 2012) Holographic Prizm as a New Optical Element . *Optics and Spectroscopy*, Vol.108(5), pp.824-830; Vol.112(2), pp. 312-317.
- [3] Chu, R.-Sh. & Tamir (1976). *J. Opt. Soc. Am.*, Vol. 66(3,12), pp. 220-226, 1438-1440
- [4] Collier, R.J. et al (1971). *Optical holography*, Academic Press, New York and London
- [5] Denisyuk, Yu.N. (1962). *Doclady AN SSSR*, Vol.144(6), pp. 522;
- [6] Denisyuk, Yu.N. & Protas, I.R. (1963). *Opt. and Spectrosc.*, Vol.14, pp. 721, USSR
- [7] Efimov, O.V. et al (2004). High efficiency volume diffractive elements in photo-thermo-refractive glass. *US Patent*. 6,673,497 B2.
- [8] Glebov, L.B. et al (1990). *Doclady AN SSSR*, Vol.314(4), pp.849-853
- [9] Hsu, K.Y. et al (2003). *Opt. Eng.*, Vol.42(5), pp. 1390-1396
- [10] Kogelnik, H. (1969). *The Bell System Technical Journal*, Vol.48, No9, P.2909-2947.
- [11] Korzinin, Yu.L. (1990), *Optics and Spectroscopy*, Vol.68(1,5), pp. 213-215, 1154-1160
- [12] Lashkov, G.I. & Sukhanov, V.I. (1978). *Optics and Spectroscopy*, Vol.44, pp. 590-594
- [13] Lin, S.N. et al. (2000). *Optics Letters*, Vol.25(7), pp. 451-453
- [14] Liu, D. et al. (2010). *Optics Express*, Vol.18(7), pp. 6447-6454
- [15] Luo, Yu. et al. (2008). *Optics Letters*, Vol.33(6), pp. 566-568
- [16] Malitson, I.H. (1963). A redetermination of some optical properties of calcium fluoride, *Appl. Opt.*, Vol.2, p. 1103
- [17] Pandey, N. et al. (2008). *Optics Letters*, Vol.33(17), pp. 1981-1983
- [18] Shcheulin, F.S. et al (2007). *Optics and Spectroscopy*, Vol.103(3,4), pp. 496; 664; 668; 673.
- [19] Shelby, R.M. (2002). Materials for holographic digital data storage, *Proceedings of SPIE*, Vol.4659, pp. 344-360
- [20] Sidorovich, V.G. (1976), *J. Technical Physics*, Vol.46(6), pp. 2168-2174, USSR

- [21] Sidorovich, V.G. (1977), *Optics and Spectroscopy*, Vol.42(4), pp. 693-699
- [22] Sidorovich, V.G. (2012), *Optics and Spectroscopy*, Vol.112(2), pp. 335-342
- [23] Steckman, G.J. et al. (1998), *Opt. Lett.*, Vol.23(16), pp. 1310-1312
- [24] Sukhanov, V.I. et al. (1984). Three dimensional hologram on Reoksan as narrow band spectral selector, *Sov. Techn. Phys. Lett.*, Vol.10, pp. 387-390
- [25] Sukhanov, V.I. et al (1992). *Optics and Spectroscopy*, Vol.72(3), pp. 716-730
- [26] Sukhanov, V.I. (1994). 3-Dimensional Deep Holograms and Materials for Recording Them, *J. Opt. Technol.*, Vol.61(1), pp. 49-56
- [27] Sukhanov, V.I. et al. (2007). *Proceedings of meeting "In Memorial of Yu.N Denisyuk "*, Sankt-Petersburg, pp. 262-276
- [28] Veniaminov, A.V. et al. (1991). *Optics and Spectroscopy*,. Vol.70, pp. 505-508
- [29] Weber, M.J. (Ed) (2003). *Handbook of Optical Materials*, CRC Press LLC
- [30] Yu, D. et al. (2010). *Optics Communs*, V.283, pp. 4219-4223
- [31] Zeldovich, B. et al. (1986). *Physics-Uspekhi*, Vol.149(3), pp. 511-549
- [32] Zlatov, A.S. et al. (2010) , *J. Opt. Technol.*, Vol.77(12), pp. 22-24